Energy Self-Sufficient Node with Integrated Lightpath Monitoring for Spectrum-Aware PON

Bernhard Schrenk, *Member, IEEE*, Markus Hofer, *Student Member, IEEE,*
Michael Hentschel, and Thomas Zemen, *Senior Member, IEEE*

***Abstract*—A reconfigurable yet energy self-sufficient signal distribution node with extensive transmission and monitoring functionalities supporting physical-layer flexibility is presented and experimentally evaluated. Operation in three different modes of wavelength distribution is supported from the O- to the L-band and features either coarse, dense wavelength or power splitting. The node does not require a local power supply unit due to the use of optical energy transmission at a delivered optical feed of -10 dBm and can be therefore deployed in a fully passive optical network. The transmission performance has been verified for analogue radio-over-fiber connectivity. Negligible penalties have been experienced when inserting the node in a realistic access network scenario, thus evidencing the absence of severe crosstalk even in case of a large number of 43 simultaneously transmitted wavelength channels. Fast switching of 10 ms long burst packets is also supported by the node. Moreover, coarse spectral monitoring of lit channels has been integrated.**

***Index Terms*— Optical fiber communication, Optical switches, Optical fiber networks, Energy harvesting, Dynamic resource allocation, Passive optical networks**

I. Introduction

THE EMERGENCE of the fifth generation (5G) of radio communications and its anticipated ~100-fold increase in delivered mobile bandwidth puts optical access and fronthaul networks into the spotlight [1]. The dynamicity in densified radio networks incorporating novel beam-centric concepts demand a flexible and sliceable optical infrastructure in order to fully exploit the consolidation strength of passive optical networks (PON). Such a virtualizable infrastructure builds on reconfigurable components. However, in case of optical access this functionality is mostly implemented in the electrical domain, while "dumb" pipes remain at the physical optical layer: Stringent requirements for passive outside fiber plants prevent the placement of electrically powered equipment offering a higher degree of network flexibility. As a possible solution reconfigurable nodes based on electro-optical switches and energy harvesting mechanisms have been recently proven feasible [2], [3]. Moreover, energy scavenging has been exploited to monitor the presence of signals traversing the PON [4].

In this work we experimentally demonstrate a shape-shifting node featuring reconfigurability in its split dimension in order to switch from a power- to a wavelength-distributing network element. Reception penalties of less than 1 dB have been found in combination with analogue radio-over-fiber transmission. Compatibility with switching of 10 ms bursts is demonstrated. We further integrate spectral monitoring functionality at a spectrally coarse level. All node functions are realized in a, from a network point-of-view, fully passive manner by means of energy harvesting, which in virtue of its low optical feed of -10 dBm enables operation of the node through a centralized power supply. To our knowledge this is the first demonstration of a remotely optically powered bidirectional network node incorporating all the aforementioned transmission and monitoring functionalities.

II. Reconfigurable Signal Distribution Node

With reach extension and integration of wireless networks fiber-optic networks in the access domain become a central pillar of the telecommunication ecosystem. As a result of collapsing different networks over the same optical distribution infrastructure, a multitude of services with highly varying demands for transmission capacity and quality-of-service are to be transported in co-existence – at low cost and high energy efficiency. Flexible and resilient networking with integrated performance monitoring is therefore paramount. However, it also constitutes a fairly exercise when to be realized under the stringent cost restrictions of optical access. One possible solution is to exploit energy harvesting to leverage the reconfigurability of originally rigid physical-layer assets such as splitters or fixed-wavelength multiplexers.

Figure 1 illustrates the architecture of the flexible 1:16 signal distribution node together with the experimental test-bed. The node can be reconfigured among a colorless 1:16 split, coarse and dense wavelength division multiplexing (CDWDM, DWDM) modes from the O- to the L-band. The CWDM mode is intended for WDM point-to-point overlay for which the channels of 1310, 1530, 1550 and 1570 nm are assigned to the four output branches. In the case of DWDM each of the drop branches is fed by a pair of 100G and 400G spaced channels at 1550 and 1530 nm, respectively, similar as

Manuscript received September 26, 2016. This work was supported in part by the European Commission through the FP7 Marie Curie Career Integration Grant WARP-5 (n° 333806).

The authors are with AIT Austrian Institute of Technology, Department of Digital Safety&Security, 1220 Vienna, Austria (e-mail: bernhard.schrenk@ait.ac.at, phone: +43 50550-4131; fax: -4190).

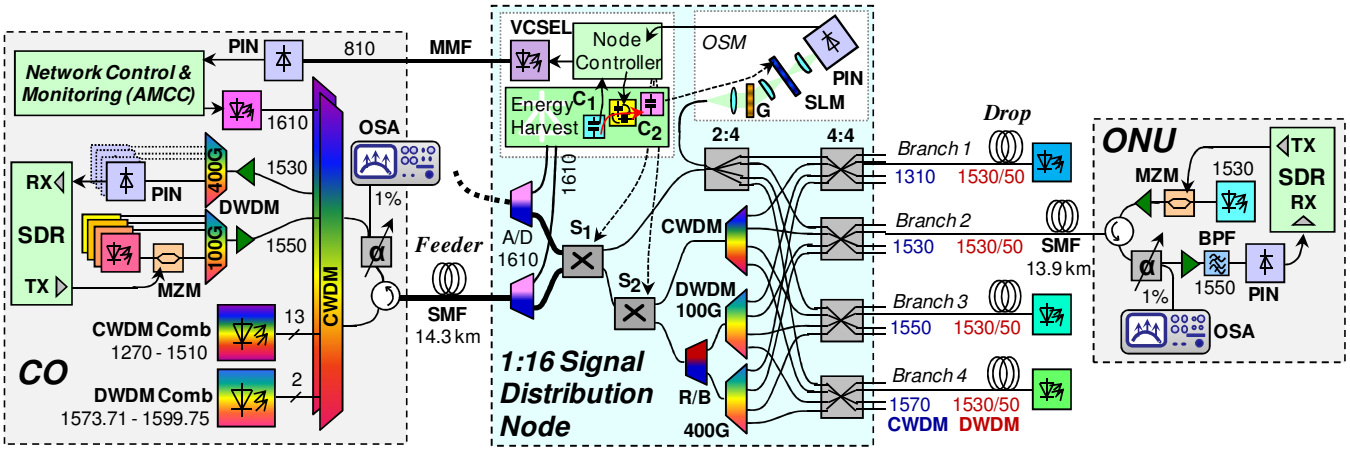

Fig. 1. Architecture of the reconfigurable 1:16 signal distribution node and experimental test-bed.

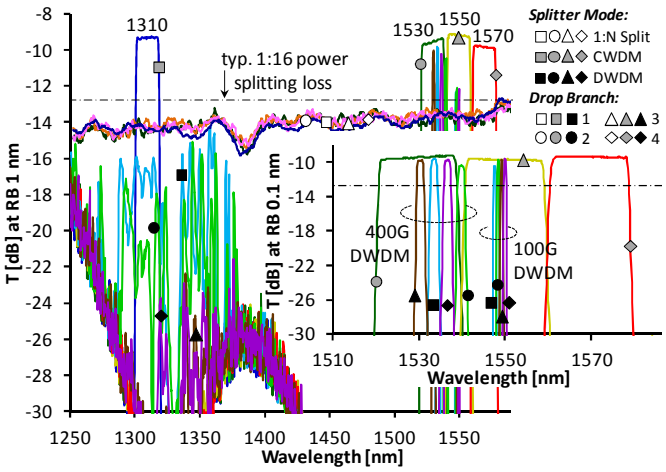

Fig. 2. Transfer functions for various splitting modes.

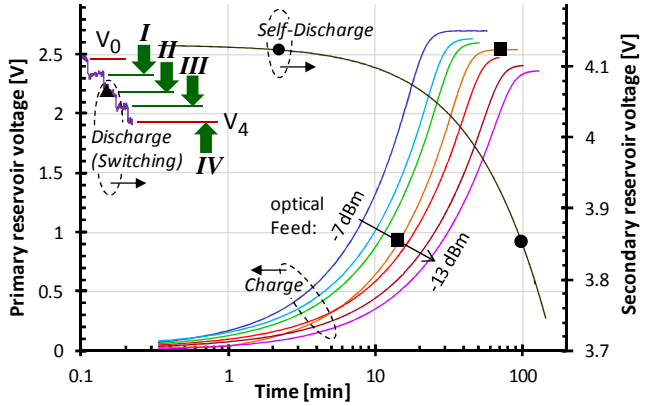

Fig. 3. Energy harvesting and depletion procedures.

in next-generation PON (NG-PON2) standards. Physical-layer reconfigurability is introduced by means of micro opto-electro-mechanic system (MOEMS) technology. Two latching 2×2 MOEMS switches (S_1, S_2) are used in combination with a low-power node controller with a steady-state power consumption of less than 3 µW, and an opto-electronic energy harvester. The respective scavenging system includes a charge reservoir connected to all MOEMS switches, which is charged by a 1×6 PIN stack and a boost converter [3]. The number of required MOEMS switches is solely determined by the number of operational modes rather than output ports. Fixed WDM filters, a red/blue (R/B) waveband filter and 4×4 star couplers provide filtering and signal distribution within the node. The star couplers at the output of the node further enable partial sharing of spectrum among multiple users. Moreover, the node is in principle laid out to perform resiliency switching (S_1) through its dual feeder port. The auxiliary management and control channel (AMCC) which also feeds the node at a level of -10 dBm was implemented at 1610 nm.

The network was further loaded with CWDM and DWDM combs covering the range from 1270 to 1610 nm. The combs were carrying dummy traffic over 43 channels and include further four closely spaced down-/upstream channels at 1530 and 1550 nm. Feeder and drop spans were each ~14 km long.

III. Node Transfer Function and Splitting Modes

Figure 2 shows the transfer function for all drop branches and various modes of operation. In the 1:N split mode a power split configuration is provided for full wavelength flexibility (□,○,Δ,◊). Extended operation at the O- and E-bands is feasible due to the broad spectral response of the MOEMS switches. The excess loss with respect to a typical 1:16 power split is 1.4 dB in average. It includes the insertion loss of a MOEMS switch, which was <0.6 dB from O- to L-band, and can be further minimized in case of a fully spliced node.

Lower pass-through losses are provided through two WDM modes. In the case of CWDM operation the node loss amounts to 9.3 to 9.8 dB and includes the insertion loss of two MOEMS switches, a red/blue (R/B) filter and a 1:4 power split. The 3-dB passband width of 17.6 nm for a CWDM channel suits WDM point-to-point overlay as it is likely to be used for 5G fronthauling.

The DWDM mode follows a spectral layout similar to that endeavored in NG-PON2. A pair of C-band wavelengths is attributed to each of the drop branches (see inset in Fig. 2), e.g., 1533.86 and 1547.72 nm in case of drop branch 1 (■). While the 100G DWDM channel around 1550 nm is intended for downstream transmission, the 400G channel around 1530 nm suits upstream transmission tolerant to wavelength drift. The insertion loss in DWDM mode is 9.7 to 10.5 dB. It shall be noted that the DWDM filters used in this experiment do not

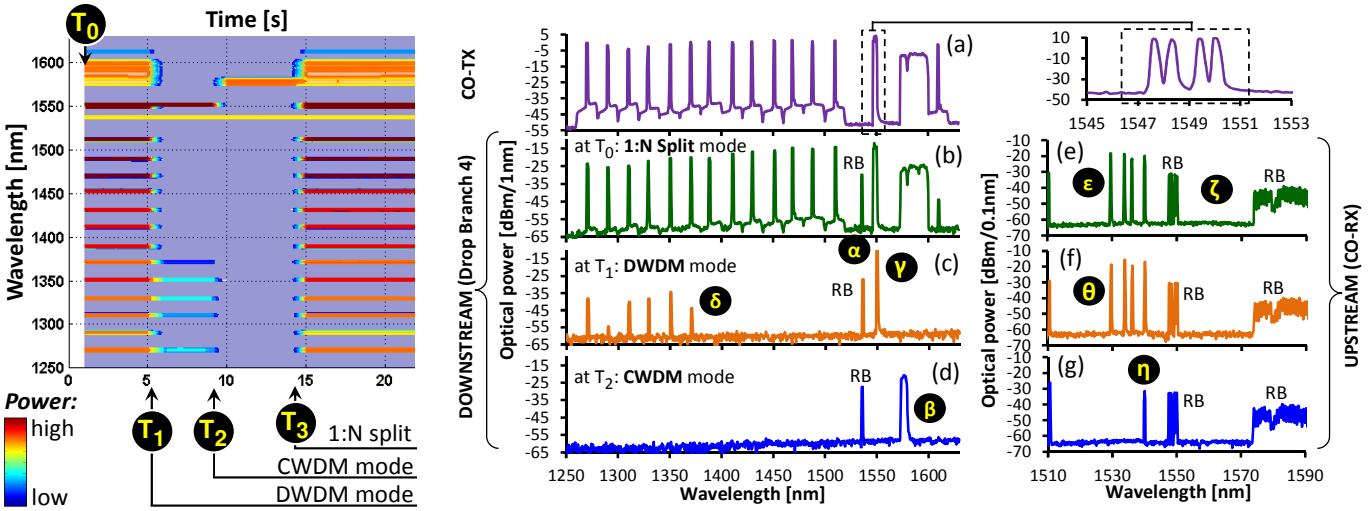

Fig. 4. Switching of the signal distribution configuration as instructed by the control plane. Measurements are shown at drop branch 4.

guarantee broadband rejection towards the O-band (■,●,▲,♦ in Fig. 2 and to be later recognized in Fig. 4(c)).

IV. Energy Scavenging

In order to supply the signal distribution node with the required energy during reconfiguration and monitoring an opto-electronic feed has been implemented [3]. Optically supply energy is harvested by PIN photodiodes in photovoltaic mode, stored in a primary reservoir (C_1) composed by a 22 mF supercapacitor and subsequently transferred to a secondary 10 mF supercapacitor (C_2) through timed boost conversion. In this way a secondary supply rail at >4V can be generated while depletion and leakage at this stage is decoupled from the first supply rail (> 1.6V) at which the node controller is connected. Figure 3 shows characteristic charge and discharge sequences at primary and secondary energy reservoirs. First, the primary reservoir is initially charged (■) and builds up the supply rail for the node controller. This takes about 26 min at an optical feed of -10 dBm. The controller then times the boost conversion from C_1 to C_2 in order to establish the higher-voltage rail at which the MOEMS switches and the spectral monitor are fed from. Due to self-discharge of the respective supercapacitor (●), which amounts to 4.3% after a period of 1 hour, burst-wise boost conversion from the primary to the secondary reservoir is required. Another source of depletion stems from switching operations (▲). In case of a charged secondary reservoir, characterized through its voltage V_0 of 4.13V, four switching operations (*I-IV*) can be performed until the secondary reservoir voltage has depleted to a level V_4 just above the operational threshold of 4V for the MOEMS switches. Recharging is then required and takes about 7 min at a feed of -10 dBm to reach the initial level V_0.

V. Reconfigurability and Burst Switching

Figure 4 presents reconfiguration of the splitting function at drop branch 4 in Figs. 4(b)-(d) and the receiver at the central office (CO) in Figs. 4(e)-(g). In the initial 1:N split mode all channels transmitted by the CO (Fig. 4(a)) are broadcasted (Fig. 4(b)), while the upstream of all 4 drop branches (ε) is received (Fig. 4(e)). Rayleigh backscattering (RB) of downstream (ζ) and upstream (α) channels can be observed. At time T_1 the node is instructed to DWDM mode and flips MOEMS switch S_1 (Figs. 4(c) and 4(f)). Only a single downstream wavelength in the 1550 nm region (γ) is forwarded to the drop branch, while all 4 upstream signals from all the drop branches are delivered to the CO receiver (θ). At T_2 the node is remotely set to CWDM mode and flips MOEMS switch S_2 (Figs. 4(d) and 4(g)). The WDM overlay at 1570 nm (β) is now forwarded in downstream direction. In upstream direction the 1530 nm DWDM channels are in principle rejected in this mode. However, since drop port 2 is assigned to the 1530 nm CWDM channel, a single upstream channel (η) is partially received by the CO as it falls on the filter edge at 1540.16 nm. At T_3 the node configuration is finally reverted to a 1:N split by toggling MOEMS switch S_1 again. This static switching application within PONs is compatible with the aforementioned energy recharge times.

Agile switching of short data bursts is further demonstrated by instructing the node to switch between DWDM and CWDM modes. With this traffic dynamics can be addressed, e.g., when WDM overlay is temporarily required for local hot-spots. Figure 5(a) shows a switching procedure monitored at drop branch 4 for inserting a burst of 10 ms conveyed over WDM overlay. The AMCC channel at 1610 nm (A) first instructs the node. The current DWDM setting (λ_1 = 1550.12 nm) is then changed to CWDM (λ_2 = 1574.54 nm) by toggling MOEMS switch S_2 (B). After the burst passed, the node is reset to DWDM operation (C). The switching time between WDM modes is ~200 µs. The capability to reconfigure and reset the node within short timescale evidences the support for agile burst switching – despite its passive nature.

VI. Transmission Performance

Whenever a large number of optical channels are spectrally processed in wavelength-selective nodes, crosstalk can impair transmission channels that are carrying fragile optical signals. High isolation to adjacent and far channels and high directivity is therefore paramount for the switching elements found within such a node. In order to demonstrate the co-existence of WDM channels for the given scenario, an analogue radio-

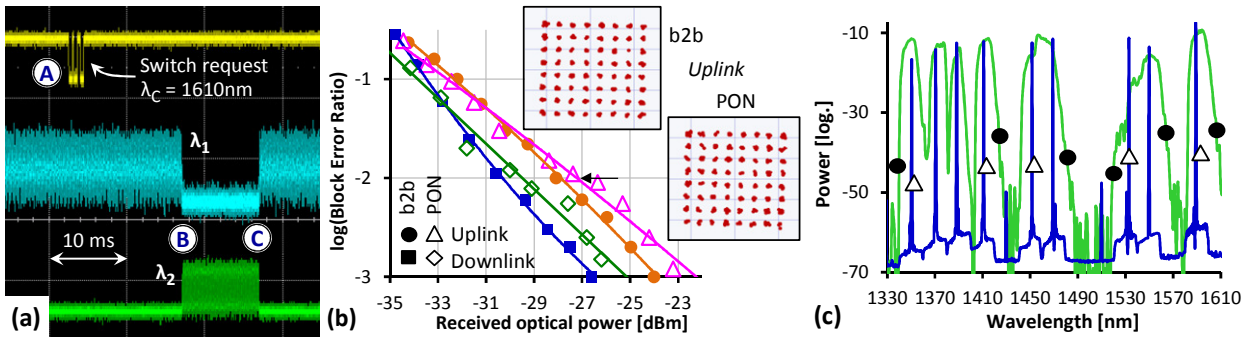

Fig. 5. (a) Dynamic burst switching. (b) Radio-over-fiber BLER performance. (c) Spectral monitoring with the integrated OSM.

over-fiber signal, which by its nature is sensitive to crosstalk effects, has been transmitted in both, down- and uplink direction. The transmission performance was assessed in terms of real-time block error ratio (BLER) measurements in combination with the NI USRP-2953R software-defined radio (SDR). A 72 Mb/s orthogonal frequency division multiplexed (OFDM) signal employing 64-ary quadrature amplitude modulation (QAM) on its subcarriers was modulated on carriers at 2.437 (downlink) and 2.457 GHz (uplink) and transmitted bidirectionally on a pair of DWDM wavelengths. The OFDM signals had 52 sub-carriers and occupied a bandwidth of 20 MHz. The code rate was 3/4. The optical transceivers comprised $LiNbO_3$ Mach-Zehnder modulators (MZM) and optically pre-amplified detectors based on an Erbium-doped fiber amplifier (EDFA) and a PIN-photodiode. Down- and uplink signals were launched with 6 dBm.

Figure 5(b) shows the BLER performance for back-to-back transmission between optical transmitter and receiver and over PON incorporating fiber spans and the node in 1:N mode. A low BLER of 10^{-3} can be obtained in all cases, which is evidenced by the clean constellation diagrams. A penalty of less than 1 dB is experienced at a BLER of 10^{-2}. This confirms the absence of severe crosstalk effects within the node, which does therefore not limit the number of supported ONUs per PON. The obtained sensitivity of -27 dBm suits to a GPON class B+ budget of 28 dB, leaving a margin of more than 5 dB.

VII. Integrated Monitoring of Lit Channels

Finally, monitoring functionality has been introduced to the signal distribution node. The aim was to extend the concept of acquiring the network status within the optical distribution network from simple power measurement at specific drop or feeder ports to spectral monitoring. The setup of the optical spectrum monitor (OSM) within the node is included in Fig. 1. The drop-side signal is coupled to a free-space optical grating (G) featuring 300 lines/mm, followed by a spatial amplitude filter composed by a liquid-crystal based spatial amplitude-only light modulator (SLM) with a resolution of 128×64 pixels. Through the SLM the node controller is able to determine the spectral slice that is detected by the low-frequency PIN detector of the OSM [5]. The acquired data of a wavelength sweep is then backhauled to the CO. For this purpose a burst transmitter based on a vertical cavity surface emitting laser diode (VCSEL) with a low-drive of 2.3 mA is connected to the node controller. Since no device in the 1550 nm region was available, a multi-mode link at 810 nm was used. The SLM had a low power consumption of 240 µA at 3.3V. A full sweep including acquisition and backhauling depletes the energy reservoir by 10%. Periodic sweeping can be facilitated after recharging the reservoir accordingly. A random selection of CWDM channels with a nominal power of -10 dBm/λ was fed into drop branch 2 to evaluate the OSM.

Figure 5(c) presents a spectrogram acquired by the OSM (●) together with an acquisition of an optical spectrum analyzer having a resolution bandwidth of 0.1 nm (Δ). The actual spectrum of the lit CWDM channels can be retrieved with good accuracy. Given the characteristics for grating and SLM, the spectral resolution of the OSM is limited by the length of the free-space lightpath in between, which was 14 cm. This also affects the acquisition when a channel falls in between spectral bins of the OSM, as in case of the 1530 nm channel (Δ), whose power is spread to two adjacent bins (●).

VIII. Conclusion

A spectrally reconfigurable wideband signal distribution node has been demonstrated. Virtual passive operation was obtained by means of energy scavenging at feed of -10 dBm implemented through re-use of the AMCC wavelength channel. The opto-electronic energy transfer enables, amongst reconfiguration of CWDM, DWDM and power splitting modes, the agile switching of 10 ms bursts. Analogue radio-over-fiber transmission of OFDM-64QAM signals did not indicate penalties due to severe crosstalk, even in presence of 43 spectral side-channels. For the first time a spectrally coarse monitor that resembles lit CWDM channels was integrated in a network node based on energy harvesting concepts.

References

[1] F. Boccardi, R.W. Heath, A. Lozano, T.L. Marzetta, P. Popovski, "Five Disruptive Technology Directions for 5G," *IEEE Comm. Mag.*, Vol. 52, no. 2, pp. 74-80, 2014.

[2] Y. Bi, J. Jin, L.G. Kazovsky, "First Experimental Demonstration of a Remotely Powered Quasi-Passive Reconfigurable Node," *IEEE Phot. Technol. Lett.*, Vol. 27, no. 9, pp. 990-993, 2015.

[3] B. Schrenk *et al.*, "Passive ROADM Flexibility in Optical Access with Spectral and Spatial Reconfigurability," *IEEE J. Sel. Areas in Comm.*, Vol. 33, no. 12, pp. 2837-2846, 2015.

[4] P. Iannone *et al.*, "High-Split Intelligent TWDM PON Enabled by Distributed Raman Amplification," in *Proc. ECOC'16*, Dusseldorf, Germany, Sept. 2016, paper Th.3.C.6.

[5] G. Baxter *et al.*, "Highly programmable Wavelength Selective Switch based on Liquid Crystal on Silicon switching elements" in *Proc. OFC'06*, Anaheim, United States, Mar. 2006, paper OTuF2.